Creep Behavior, Deformation Mechanisms, and Creep Life of Mod.9Cr-1Mo Steel

FUJIO ABE

The creep behavior, deformation mechanisms, and the correlation between creep deformation parameters and creep life have been investigated for Mod.9Cr-1Mo steel (Gr.91, 9Cr-1Mo-VNb) by analyzing creep strain data at 723 K to 998 K (450 °C to 725 °C), 40 to 450 MPa, and t_r = 11.4 to 68,755 hours in NIMS Creep Data Sheet. The time to rupture t_r is reasonably correlated with the minimum creep rate $\dot{\varepsilon}_{min}$ and the acceleration of creep rate by strain in the acceleration region $d\ln\dot{\varepsilon}/d\varepsilon$, as $t_r = 1.5/[\dot{\varepsilon}_{min}\,(d\ln\dot{\varepsilon}/d\varepsilon)]$, where $\dot{\varepsilon}_{min}$ and $d\ln\dot{\varepsilon}/d\varepsilon$ reflect the creep behavior in the transient and acceleration regions, respectively. The $\dot{\varepsilon}_{min}$ is inversely proportional to the time to minimum creep rate t_m, while it is proportional to the strain to minimum creep rate ε_m, as $\dot{\varepsilon}_{min} = 0.54\ (\varepsilon_m/t_m)$. The ε_m decreases with decreasing stress, suggesting that the creep deformation in the transient region becomes localized in the vicinity of prior austenite grain boundaries with decreasing stress. The duration of acceleration region is proportional to the duration of transient region, while the $d\ln\dot{\varepsilon}/d\varepsilon$ is inversely proportional to the ε_m. The t_r is also correlated with the t_m, as $t_r = g\,t_m$, where g is a constant. The present creep life equations reasonably predict the degradation in creep rupture strength at long times. The downward deviation takes place in the t_r *vs* $\dot{\varepsilon}_{min}$ curves (Monkman–Grant plot). At the same $\dot{\varepsilon}_{min}$, both the ε_m and t_m change upon the condition of $t_m \propto \varepsilon_m$. The decrease in ε_m with decreasing stress, corresponding to decreasing $\dot{\varepsilon}_{min}$, causes a decrease in t_m, indicating the downward deviation of the t_r *vs* $\dot{\varepsilon}_{min}$ curves.

DOI: 10.1007/s11661-015-3144-5

I. INTRODUCTION

TEMPERED martensitic 9 to 12 pct Cr steels have been favored as creep strength-enhanced ferritic (CSEF) steels for application to thick section boiler and turbine components of coal-fired ultra-supercritical (USC) power plants[1,2] with steam temperature at around 873 K (600 °C) and also for application to future fast breeder nuclear reactor.[3] 9 to 12 pct Cr steels such as Mod.9Cr-1Mo steel specified as ASME Gr.91 (9Cr-1Mo-0.2V-0.05Nb) can offer the highest potential to meet the required flexibility for USC power plants, because of their smaller thermal expansion and larger thermal conductivity than austenitic steels and Ni base superalloys. At present, Gr.91 is one of the most popular CSEF steels widely used in USC power plants.[4]

A deciding criterion for creep resistance of USC power plant steels is usually 100,000 hours creep rupture strength at operating temperature.[5] The 100,000 hours creep rupture strength is usually estimated by extrapolation using short-term creep rupture data. But it becomes evident that the stress rupture data of CSEF steels sometimes exhibit an inflection indicating the degradation in creep strength at long times and that the conventional time–temperature–parameter (TTP) methods such as Larson–Miller parameter method could not evaluate long-term creep life correctly but tended to overestimate it.[1,6,7] The stress extrapolation makes it difficult to evaluate long-term creep life of CSEF steels correctly. The new analysis methods, such as International Standard Organization Creep Rupture Data Assessment (ISO CRDA) method,[8] Wilshire and Sharning method,[9] region splitting analysis method,[10] and multi-region analysis method,[11] have been proposed as more reliable methods than the conventional TTP methods.

For the improvement of reliability of long-term creep life estimation for Gr.91, efforts have also been paid to clarify the correlation between creep life and creep deformation behavior by the analysis of creep strain data.[4] There is an ever evolving microstructure in tempered martensitic 9 to 12Cr steels and the change in creep rate with time and strain reflects coupled elementary processes during creep, such as micro-grain growth, change in dislocation density, and change in precipitate volume fraction and size.[12] This implies that the creep strain behavior can be reasonably correlated with the creep life. The creep and creep rate curves provide us fundamental but very useful information on life assessment as well as on creep deformation mechanisms.

The Omega method has successfully been applied to the remaining creep life estimation of Gr.91.[13,14] Prager proposed the Omega method for prediction of

FUJIO ABE, Research Fellow, is with the Materials Reliability Unit, Environment and Energy Materials Division, National Institute for Materials Science (NIMS), 1-2-1 Sengen, Tsukuba 305-0047, Japan. Contact e-mail: ABE.Fujio@nims.go.jp
Manuscript submitted February 9, 2015.
Article published online September 21, 2015

remaining life of service exposed materials.[15] The remaining creep life at a time t in the acceleration creep region is inversely correlated with Omega parameter $\Omega = d\ln\dot{\varepsilon}/d\varepsilon$, where $\dot{\varepsilon}$ and ε are the creep rate and creep strain, respectively, at a time t. Semba and co-workers applied a microstructure-based continuum creep damage mechanics (CDM) model to describe the creep strain behavior and to estimate the creep life of Gr.91.[16] Lim, Sauzay, and co-workers analyzed an increase in creep rate in the acceleration creep region of Gr.91 and proposed a necking model for prediction of the creep life.[17] Abe and co-workers have analyzed the creep strain data of 9Cr and austenitic steels to make clear the correlation between the creep life and creep deformation parameters.[18–20]

The purpose of the present research is to investigate the creep behavior, creep deformation mechanisms, and the correlation between the creep life and creep deformation parameters for Gr.91 by analyzing creep and creep rate curves. The results on Gr.91 are compared with those on other ferritic steels. The microstructure evolution in the present Gr.91 during creep has been reported by Kimura and co-workers.[21–23]

II. CREEP DATA AND ANALYTICAL PROCEDURE

The present author analyzed the creep data of Gr.91 in the Atlas of Creep Deformation Property no. D-1 and no. D-2,[24,25] which are another series of NIMS Creep Data Sheets. The Atlas of Creep Deformation Property contains a full set of creep data, such as instantaneous strain, time to specific strain, minimum creep rate, time to rupture, rupture elongation and reduction of area for three heats of tubes and for three heats of plates of Gr.91 in wide temperature and stress ranges of 723 K to 998 K (450 °C to 725 °C) and 30 to 450 MPa, respectively, under constant load conditions, together with many graphs showing creep curves, creep rate *vs* time curves, and creep rate *vs* strain curves. The shortest and longest times to rupture were 11.4 and 68,755 hours, respectively. The Atlas of Creep Deformation Property also contains short-time tensile data of 0.2 pct proof stress, ultimate tensile strength, elongation, and reduction of area in the temperature range between room temperature and 1023 K (750 °C), together with the materials data, such as chemical compositions, production methods of the tubes and plates, heat treatments, austenite grain size, hardness, volume fraction of non-metallic inclusions, and optical micrographs of the as-received tubes and plates.

The chemical compositions and heat treatment conditions of the tubes and plates of Gr.91 examined are given in Table I. The primary or transient creep region, where the creep rate decreases with time, is defined as the region from the beginning of creep to a time to reach minimum creep rate $\dot{\varepsilon}_{min}$, as shown in Figure 1. The tertiary or acceleration creep region, where the creep rate increases with time after reaching a minimum creep rate $\dot{\varepsilon}_{min}$, is defined as the region from a time to reach minimum creep rate to a time to rupture. There is substantially no steady-state region, where the creep rate is constant. The time to minimum creep rate t_m and the strain to minimum creep rate ε_m were evaluated from the creep rate *vs* time curves and creep rate *vs* strain curves, respectively. The increase in creep rate by strain $d\ln\dot{\varepsilon}/d\varepsilon$ in the acceleration region was evaluated from the slope of the creep rate *vs* strain curves. The $d\ln\dot{\varepsilon}/d\varepsilon$ corresponds to the β and Ω parameters proposed by Wu *et al.*[26] and by Prager,[15] respectively.

In the present paper, the tube materials denote T91 according to the ASME specification. The plate materials and all the materials containing tube and plate denote Gr.91.

III. CREEP BEHAVIOR

A. *Creep Behavior in Transient Region and Minimum Creep Rate*

The present author has revealed for tempered martensitic 9Cr steel that the transient creep is basically a consequence of the movement and annihilation of a high density of dislocations due to martensitic microstructure and that the acceleration creep is a consequence of gradual loss of creep strength due to the microstructure recovery.[27,28] The onset of acceleration creep is closely correlated with the onset of recovery of martensitic microstructure at or near prior austenite grain boundaries (PAGBs), such as the onset of migration of lath or block boundaries, causing the coarsening of the lath or block in the acceleration creep region.

Figure 2 shows the stress dependence of minimum creep rate $\dot{\varepsilon}_{min}$ for the heats MGC and MgB of Gr.91. The $\dot{\varepsilon}_{min}$ is described by a power law of

$$\dot{\varepsilon}_{min} = A\,\sigma^n, \qquad [1]$$

where A is a constant and n is the stress exponent. The stress exponent n is evaluated to be about 15 and 6 at high and low stresses, respectively, for the heats MGC and MgB, while the $\dot{\varepsilon}_{min}$ is higher in the heat MgB than in the heat MGC in the stress range examined at 823 K and 873 K (550 °C and 600 °C). The higher $\dot{\varepsilon}_{min}$ results in shorter time to rupture and lower creep rupture strength of the heat MgB than the heat MGC, as shown in Figure 3. The critical stresses dividing the high and low stresses are 184, 132, 106, and 75 MPa at 823 K, 873 K, 898 K, and 948 K (550 °C, 600 °C, 625 °C, and 675 °C), respectively, for the heat MGC, while those are 172, 123, and 85 MPa at 823 K, 873 K, and 923 K (550 °C, 600 °C, and 650 °C), respectively, for the heat MgB. The critical stresses are close to those by Kimura's region splitting analysis.[10] The stress exponent n of about 6 for the heats MGC and MgB suggests dislocation creep mode[29,30] at low stresses, which was also typical for the other heats. The lowest stresses examined were 70 and 40 MPa at 873 K and 923 K (600 °C and 650 °C), respectively, for the heat MgB.

The stress exponent n of about 6 obtained in the present work is much larger than that of $n = 1$ by Kloc and Sklenicka.[31] They carried out short-term creep tests for Gr.91 for up to about 2000 hours at

Table I. Chemical Compositions and Heat Treatment Conditions of Tubes and Plates of Gr.91 Examined

Tube									(mass pct)
	C	Si	Mn	P	S	Ni	Cr	Mo	V
Requirement	0.08 to 0.12	0.20 to 0.50	0.30 to 0.60	<0.020	<0.010	<0.40	8.00 to 9.50	0.85 to 1.05	0.18 to 0.25
MGA	0.10	0.38	0.40	0.015	0.001	0.12	8.53	0.96	0.21
MGB	0.09	0.34	0.45	0.015	0.001	0.20	8.51	0.90	0.205
MGC	0.09	0.29	0.35	0.009	0.002	0.28	8.70	0.90	0.22

	Al	N	Nb	Normalizing	Tempering
Requirement	<0.04	0.030 to 0.070	0.06 to 0.10		
MGA	0.010	0.05	0.076	1318 K (1045 °C)/10 min AC	1053 K (780 °C)/60 min AC
MGB	0.02	0.042	0.076	1323 K (1050 °C)/60 min AC	1033 K (760 °C)/60 min AC
MGC	0.001	0.044	0.072	1323 K (1050 °C)/10 min AC	1038 K (765 °C)/30 min AC

Plate									(mass pct)
	C	Si	Mn	P	S	Ni	Cr	Mo	V
Requirement	0.06 to 0.15	0.18 to 0.56	0.25 to 0.66	<0.025	<0.012	<0.43	8.00 to 9.50	0.85 to 1.05	0.16 to 0.27
MgA	0.08	0.34	0.49	0.005	0.004	0.09	8.34	0.89	0.23
MgB	0.08	0.34	0.49	0.005	0.004	0.09	8.34	0.89	0.23
MgC	0.10	0.24	0.44	0.005	0.001	0.04	8.74	0.94	0.21

	Al	N	Nb	Normalizing	Tempering
Requirement	<0.05	0.025 to 0.080	0.05 to 0.11		
MgA	0.011	0.059	0.070	1323 K (1050 °C)/10 min AC	1043 K (770 °C)/60 min AC, 1013 K (740 °C)/8.4 h FC
MgB	0.011	0.059	0.070	1323 K (1050 °C)/10 min AC	1043 K (770 °C)/60 min AC, 1013 K (740 °C)/60 min FC
MgC	0.014	0.0582	0.076	1333 K (1060 °C)/90 min AC	1033 K (760 °C)/60 min AC, 1003 K (730 °C)/8.4 h FC

temperatures from 873 K to 923 K (600 °C to 650 °C) and at low stresses below 100 MPa by means of a helicoid spring specimen technique. Since the stress and strain in helicoid spring are essentially shear ones, they were transformed to the equivalent tensile quantities. In order to estimate the steady-state creep rate, the creep curves were fitted by an equation proposed by Li.[32] The estimated steady-state creep rates are proportional to applied stress from about 1 MPa up to about 100 MPa at 873 K (600 °C), indicating the stress exponent n of steady-state creep rate is 1, suggesting diffusional creep. The transition from power-law creep with $n \approx 10$ to the diffusional creep is found at stresses around 100 MPa at 873 K (600 °C). Recently, Yamasaki and co-workers reported the similar results for Gr.91.[33] They carried out short-term creep tests for up to about 75 hours at 823 K to 923 K (550 °C to 650 °C) by a helicoid spring specimen technique and estimated the $\dot{\varepsilon}_{min}$ by curve fitting using an equation proposed by Li.[32] The stress exponent of $\dot{\varepsilon}_{min}$ is evaluated to be 1 at stresses below 130, 85, and 70 MPa at 823 K, 873 K, and 923 K (550 °C, 600 °C, and 650 °C), respectively. It should be noted that the effect of microstructure evolution during creep is ignored in their estimation of steady-state creep rate or $\dot{\varepsilon}_{min}$. In NIMS Creep Data Sheets, on the other hand, the creep strain was continuously measured for up to final rupture during creep test and the $\dot{\varepsilon}_{min}$ was obtained from the creep rate curves without any extrapolation nor any curve fitting. The time to minimum creep rate t_m was 1.2×10^4 hours at 873 K (600 °C) and 70 MPa, and 9.0×10^3 hours at 923 K (650 °C) and 40 MPa for the heat MgB, which were much longer than the duration of creep tests by Kloc and Sklenicka and by Yamasaki and co-workers.

The minimum creep rate $\dot{\varepsilon}_{min}$ is inversely proportional to the t_m as shown in Figure 4 and is given by

$$\dot{\varepsilon}_{min} = 1.0 \times 10^{-2}/t_m. \quad [2]$$

The relationship between the $\dot{\varepsilon}_{min}$ and t_m is described by a unique line given by Eq. [2], irrespective of the different heats and different temperatures. The different heats exhibit different $\dot{\varepsilon}_{min}$ and different creep rupture strength, as shown in Figures 2 and 3. The inverse proportionality between the $\dot{\varepsilon}_{min}$ and t_m was already reported for Gr.91 by Spigarelli *et al.*[34] They carried out creep tests for Gr.91 at 848 K, 873 K, 898 K, and 923 K (575 °C, 600 °C, 625 °C, and 650 °C), where the longest time to rupture was about 3500 hours, and found the inverse proportionality between the $\dot{\varepsilon}_{min}$ and t_m in the range of t_m between 3 and 700 hours. Eq. [2] with different proportional constant of 1.8×10^{-2} was also reported for a tempered martensitic 9Cr-1W steel containing no MX forming elements V and Nb.[19] The

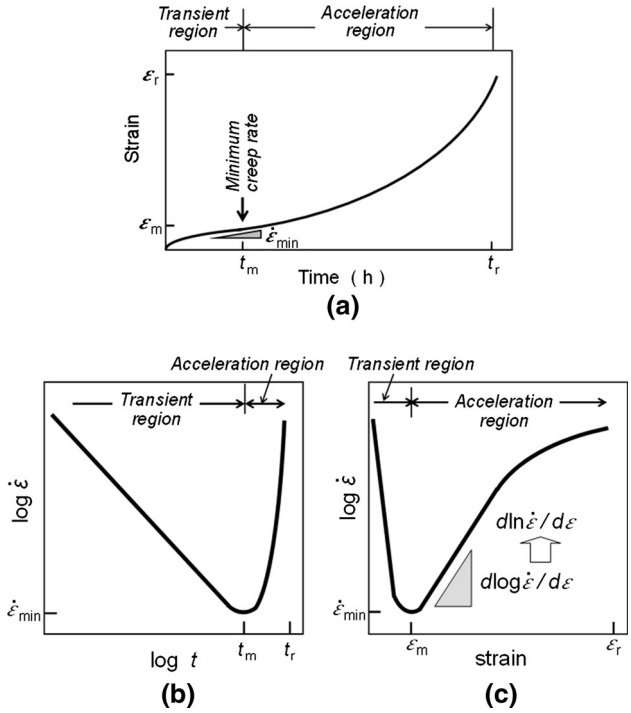

Fig. 1—(*a*) Schematic creep curve, (*b*) creep rate *vs* time curve, and (*c*) creep rate *vs* strain curve.

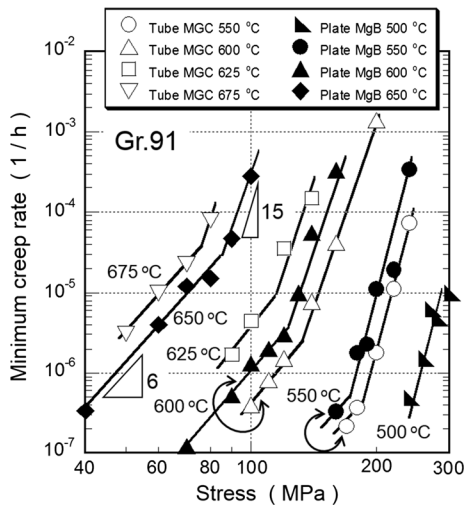

Fig. 2—Stress dependence of minimum creep rate for heats MGC and MgB of Gr.91 at 773 K to 948 K (500 °C to 675 °C).

proportional constant reflects the resistance to creep deformation. Gr.91 exhibits much lower $\dot{\varepsilon}_{min}$ than the 9Cr-1W steel at same stress conditions.

The decrease in $\dot{\varepsilon}_{min}$ with t_m becomes more significant at long times above about 5×10^3, 5×10^2, and 1×10^2 hours at 823 K, 873 K, and 923 K (550 °C, 600 °C, and 650 °C), respectively, deviating from Eq. [2]. At 773 K and 948 K (500 °C and 675 °C), no deviation from Eq. [2] is observed. The data points at 948 K (675 °C) are limited at short times less than 2200 hours in t_m. But the t_m of 2200 hours is enough to recognize no deviation from Eq. [2] at 948 K (675 °C), because the deviation appears at long times above 5×10^2 and 1×10^2 hours at 873 K and 923 K (600 °C and 650 °C), respectively. The most promising mechanism for the deviation is that the precipitation of fine Fe_2Mo Laves phase in the transient region at around 873 K (600 °C) further decreases the creep rate. The precipitation of fine Fe_2W Laves phase took place at early stage of creep in 9Cr-2W and 9Cr-4W steels at 873 K and 923 K (600 °C and 650 °C), which significantly decreased the creep rate.[20] The Fe_2Mo Laves phase can precipitate even at 773 K (500 °C) but it needs longer times above 2.7×10^4 hours, which was the longest t_m at 773 K (500 °C), because of lower temperature. The Fe_2Mo Laves phase does not precipitate at 948 K (675 °C), because of below the solubility limit.

The t_m corresponds to the onset time of acceleration creep. Based on the mechanisms that the onset of acceleration creep is closely correlated with the onset of recovery of martensitic microstructure, the t_m corresponds to the onset time of recovery of martensitic microstructure for cause of acceleration creep. This indicates that the stabilization of martensitic microstructure by fine distribution of $M_{23}C_6$ along PAGBs, and lath and block boundaries shifts the t_m to longer times, which further decreases the $\dot{\varepsilon}_{min}$ and hence increases the t_r.

The strain to minimum creep rate ε_m is evaluated to be 0.02 to 0.03 at high stresses at each temperature and it decreases with decreasing stress at temperatures above 823 K (550 °C), as shown in Figure 5. At a low temperature of 773 K (500 °C), the data on ε_m are available only at high and narrow stress range of 240 to 320 MPa and the ε_m is regarded as approximately constant of 0.01 to 0.025. The present results indicate that the onset of acceleration creep takes place when the creep strain reaches to 0.02 to 0.03 (2 to 3 pct) at high stresses. The decrease in ε_m with decreasing stress suggests that the creep deformation in the transient region becomes localized with decreasing stress. The most appropriate possibility is the preferential creep deformation in the vicinity of PAGBs at low stresses, because GB diffusion enhances the microstructure recovery in the vicinity of PAGBs. Based on the results in Figure 5 that the ε_m at low stresses is about 1/10 of that at high stresses, it is suggested that the creep deformation in the transient region is significantly localized within 1 μm, corresponding to a few laths, in the vicinity of PAGBs at low stresses.[35] Kushima and co-workers pointed out that the loss of creep strength of Gr.91 at 873 K (600 °C) and low stresses is due to the preferential recovery of lath martensitic microstructure in the vicinity of PAGBs and that the preferential microstructure recovery promotes localized creep deformation in the vicinity of PAGBs.[36] Another possibility is a loss of pinning effect during long-term creep at low stresses. The coarsening of $M_{23}C_6$ carbides and MX carbonitrides and *Z*-phase precipitation with depletion of MX carbonitrides during creep,[37–39] which result in a loss of pinning effect, also promote the onset of acceleration creep, even when the accumulated creep strain is low. This is more significant at lower stresses, because of longer time of exposure, and decreases ε_m.

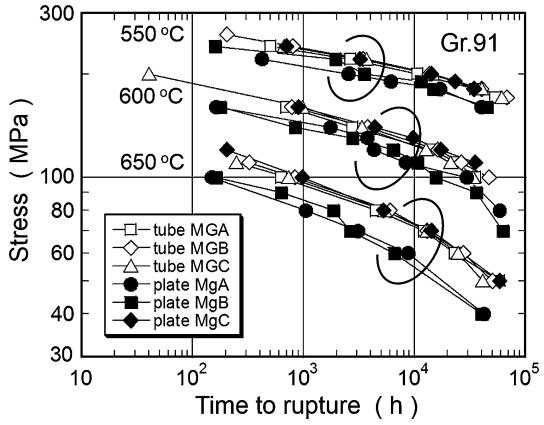

Fig. 3—Creep rupture data for tubes and plates of Gr.91.

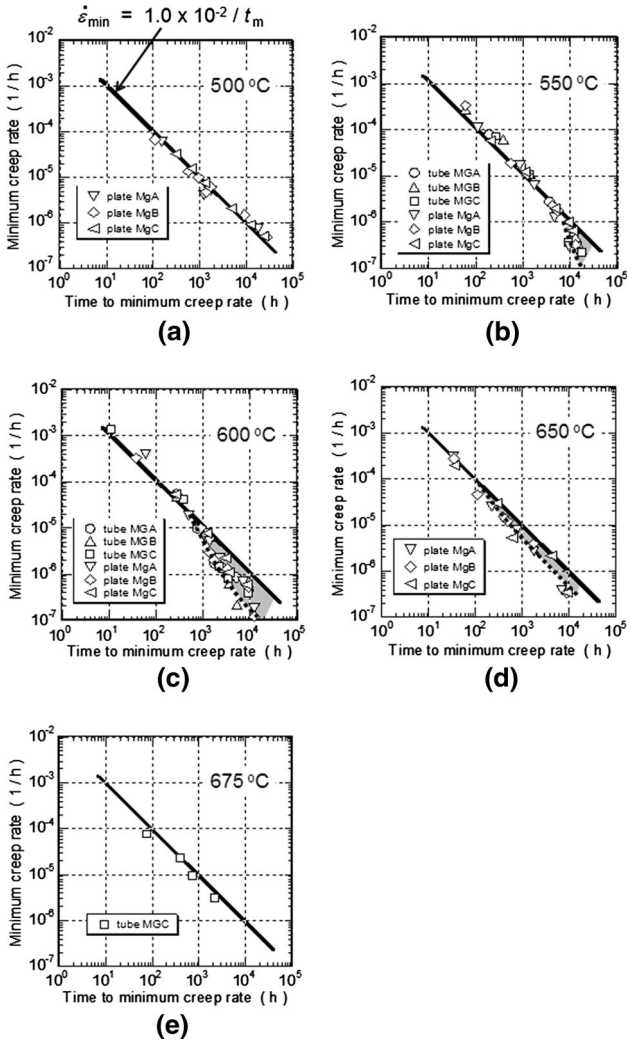

Fig. 4—Minimum creep rate as a function of time to minimum creep rate t_m for Gr.91.

While the $\dot{\varepsilon}_{min}$ decreases with increasing t_m as shown in Figure 4, it increases with increasing ε_m as shown in Figure 6. In Figure 6, the increase in ε_m in the abscissa corresponds to the increase in stress as can be seen from

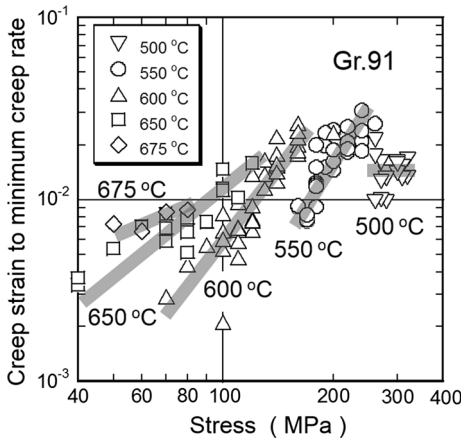

Fig. 5—Stress dependence of strain to minimum creep rate at 773 K to 948 K (500 °C to 675 °C) for Gr.91.

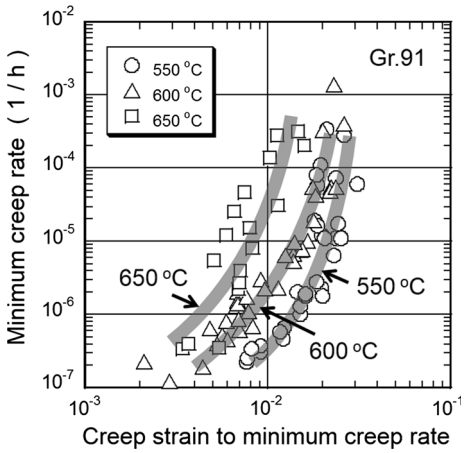

Fig. 6—Relationship between minimum creep rate $\dot{\varepsilon}_{min}$ and strain to minimum creep rate ε_m for Gr.91.

Figure 5, which shows the ε_m increases with increasing stress. Figures 4 and 6 indicate that the $\dot{\varepsilon}_{min}$ depends on both the t_m and ε_m. We obtain

$$\dot{\varepsilon}_{min} = 0.54(\varepsilon_m/t_m), \qquad [3]$$

as shown in Figure 7. With decreasing stress, the t_m increases several orders of magnitude (Figure 4) but the ε_m decreases within one order of magnitude (Figure 5). Therefore, the stress dependence of minimum creep rate is mainly due to that of t_m but not due to ε_m and hence that the retardation of onset of acceleration creep, causing an increase in t_m, is very effective for a significant decrease in $\dot{\varepsilon}_{min}$, which results in a significant increase in t_r.

B. *Creep Behavior in Acceleration Region*

Figure 8(a) shows an example of the evaluation of $d\ln\dot{\varepsilon}/d\varepsilon$ for the MGC heat at 873 K (600 °C). The $d\ln\dot{\varepsilon}/d\varepsilon$ increases with decreasing stress. The linear part of the creep rate *vs* strain curves in the acceleration region decreases with decreasing stress and is only about 50 pct of the acceleration region at low stresses of 110 and

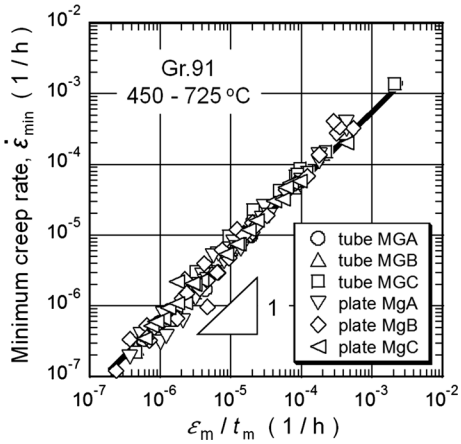

Fig. 7—Relationship between minimum creep rate $\dot{\varepsilon}_{min}$ and ε_m/t_m for Gr.91.

100 MPa. However, the linear part of the creep rate *vs* strain curves in the acceleration region corresponds to larger than 90 pct of the acceleration region in the creep strain *vs* time curves even at a low stress of 100 MPa, as shown in Figure 8(b), because the creep strain significantly increases just before the creep rupture. This suggests that the parameter $d\ln\dot{\varepsilon}/d\varepsilon$ represents the creep deformation characteristics over a greater part of acceleration region. The linear acceleration of logarithm of creep rate with strain has been reported for several Cr-Mo steels,[15,26,40] 9Cr-W steels[19,20,41,42], and austenitic steels.[43]

Assuming an exponential dependence of strain on creep rate, the creep rate in the acceleration region is described by[19,20]

$$\dot{\varepsilon} = \dot{\varepsilon}_0 \exp(n\varepsilon) \exp(m\varepsilon) \exp(d\varepsilon) \exp(i\varepsilon) \qquad [4]$$

$$d\ln\dot{\varepsilon}/d\varepsilon = n + m + d + i, \qquad [5]$$

where $\dot{\varepsilon}_0$ is the initial creep rate, n the stress exponent for the Norton's power law for minimum creep rate given by $\dot{\varepsilon}_{min} = B\sigma^n$, where B is a constant, m the microstructure degradation parameter, d the damage parameter due to creep voids, and i describes the effect of localized creep deformation. Because the microstructure observations gave no evidence of any formation of creep voids in base metal of Gr.91 showing the development of creep damage until the specimen reaches the final stage of creep rupture, corresponding to necking, the parameter d in Eqs. [4] and [5] is neglected and the $d\ln\dot{\varepsilon}/d\varepsilon$ substantially results from the parameters n, m, and i. The n, m, and i correspond to the increase in creep rate by an increase in stress due to a decrease in cross section with strain at constant load test, by a strength loss due to microstructure evolution, and by a strength loss due to localized creep deformation in the vicinity of PAGBs, respectively.

Figure 9 shows the stress and temperature dependence of $d\ln\dot{\varepsilon}/d\varepsilon$, which was evaluated from the constant portion of $d\ln\dot{\varepsilon}/d\varepsilon$ in the acceleration region shown in Figure 8, for the heat MGC of T91 and the comparison

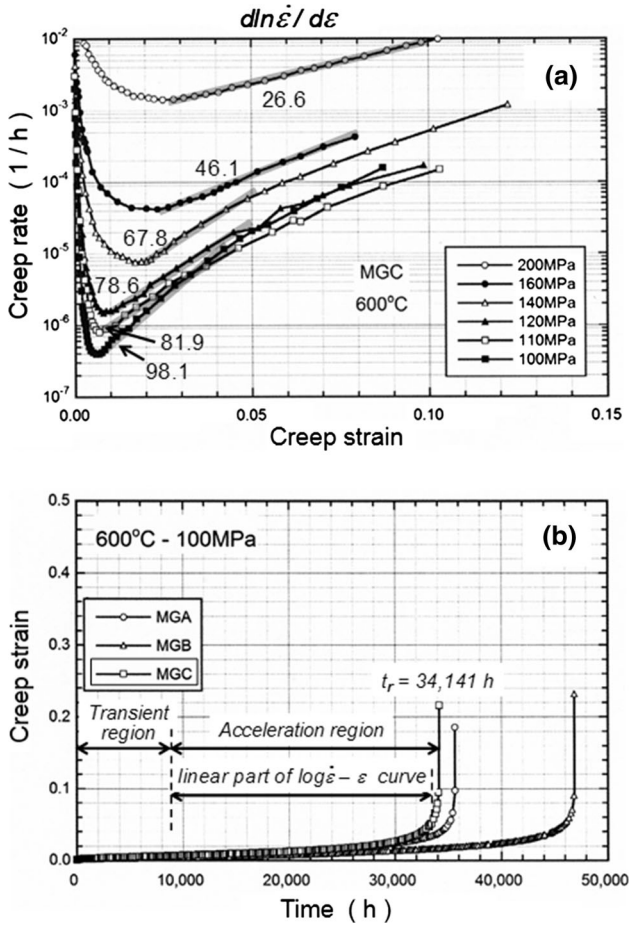

Fig. 8—(*a*) Creep rate *vs* strain curves and evaluation of $d\ln\dot{\varepsilon}/d\varepsilon$ for heat MGC of T91 at 873 K (600 °C), and (*b*) creep curves of heats MGA, MGB, and MGC at 873 K (600 °C) and 100 MPa.

between the $d\ln\dot{\varepsilon}/d\varepsilon$ and stress exponent n (Eqs. [4] and [5]) at 873 K (600 °C). At a high stress of 200 MPa at 873 K (600 °C), the $d\ln\dot{\varepsilon}/d\varepsilon$ is evaluated to be 26.6, which is a little bit larger than the stress exponent n of minimum creep rate; $n = 15$ at high stresses. Therefore, the $d\ln\dot{\varepsilon}/d\varepsilon$ mainly consists of the parameter n in Eqs. [4] and [5] at high stresses. This indicates that at high stresses the increase in creep rate in the acceleration region mainly results from an increase in stress by a decrease in cross section with strain under constant load test conditions and that the microstructure evolution effect is only a little bit for the acceleration of creep rate. With decreasing stress, the $d\ln\dot{\varepsilon}/d\varepsilon$ increases to about 100. At low stresses, the $d\ln\dot{\varepsilon}/d\varepsilon$ consists of the parameters m and i, mainly, because the value of $d\ln\dot{\varepsilon}/d\varepsilon$ is much larger than that of the parameter n of about 6 at low stresses. This indicates that at low stresses the increase in creep rate in the acceleration region mainly results from the microstructure evolution effect causing softening. Kimura and co-workers observed that recovered area extended toward inside the grain from PAGBs during acceleration creep in Gr.91 at 873 K (600 °C) and at a low stress of 70 MPa.[10]

Maruyama and co-workers reported that subgrain boundaries are the major obstacles to dislocation

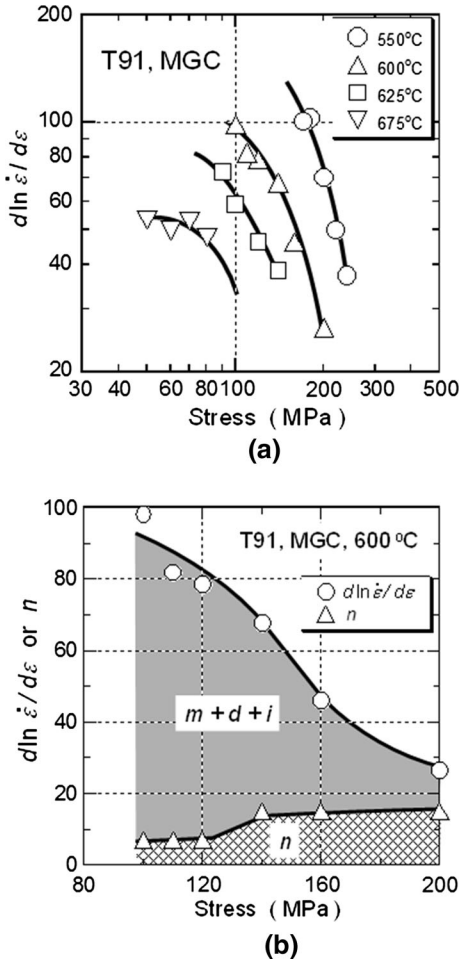

Fig. 9—(*a*) $d\ln\dot{\varepsilon}/d\varepsilon$ in acceleration creep region for heat MGC of T91 and (*b*) comparison of $d\ln\dot{\varepsilon}/d\varepsilon$ and stress exponent n at 873 K (600 °C).

motion in high Cr ferritic steels and that the creep strength of Gr.91 is mainly determined by subgrain width.[11,44] There are two types of recovery processes of subgrains which happen in Gr.91 steel during creep exposure: strain-induced recovery and static or thermal recovery. The static or thermal recovery of subgrains is caused by the loss of pinning force from $M_{23}C_6$ precipitates at boundaries. In Figure 9, the high stress region, where the $d\ln\dot{\varepsilon}/d\varepsilon$ mainly consists of the parameter n, corresponds to the strain-induced recovery region by Maruyama and co-workers. The low stress region, where the $d\ln\dot{\varepsilon}/d\varepsilon$ mainly consists of the parameters m and i, corresponds to the static recovery region by Maruyama and co-workers.

Sawada and co-workers reported the importance of stability of precipitates of $M_{23}C_6$ carbides, MX carbonitrides, and Z phase during long-term creep at low stresses for the creep strength of Gr.91 at around 873 K (600 °C).[45] They investigated the microstructure evolution in the heat MGC of present Gr.91 shown in Table I during long-term creep at 873 K (600 °C) and 70 MPa, at which the degradation in creep strength was significant, with emphasis on the Z-phase formation. The number density of Z phase gradually increases with time after about 10,000 hours, while that of MX decreases substantially after 30,000 hours. This suggests that the MX particles become dissolved with time in favor of the growth of more stable Z phase. They concluded that the preferential recovery in the vicinity of PAGBs and the abrupt decrease in number density of MX particles due to Z-phase formation contribute to the premature failure of Gr.91. Taking the results by Sawada and co-workers into account, the $d\ln\dot{\varepsilon}/d\varepsilon$ mainly consists of the parameters m and i at low stresses and the change in $d\ln\dot{\varepsilon}/d\varepsilon$ with stress reflects the stability of precipitates.

C. *Influence of Transient Creep on Subsequent Acceleration Creep*

The creep behavior in the acceleration region is not independent from that in the transient region. The $d\ln\dot{\varepsilon}/d\varepsilon$ is inversely proportional to the strain to minimum creep rate ε_m as shown in Figure 10, namely, $d\ln\dot{\varepsilon}/d\varepsilon = D/\varepsilon_m$, where D is a constant. The constant D is evaluated to be 0.87, 0.66, and 0.41 at 823 K, 873 K, and 923 K (550 °C, 600 °C, and 650 °C), respectively. Taking the temperature dependence of the constant D into account, the $d\ln\dot{\varepsilon}/d\varepsilon$ is described as

$$d\ln\dot{\varepsilon}/d\varepsilon = \left(4.66 - 4.6\times10^{-3}T\right)/\varepsilon_m, \qquad [6]$$

in the temperature range between 823 K and 923 K (550 °C and 650 °C), where T is the temperature in K. Equation [6] indicates that the homogeneous creep deformation in the transient region at high stresses, as indicated by the large values of ε_m, causes the small values of $d\ln\dot{\varepsilon}/d\varepsilon$ in the acceleration region. On the other hand, the localized creep deformation in the transient region at low stresses, as indicated by the small values of ε_m, causes the large values of $d\ln\dot{\varepsilon}/d\varepsilon$ in the acceleration region. The increase in proportional constant D with decreasing temperature suggests that the localization of creep deformation is more significant with decreasing temperature, because the localized microstructure evolution during creep due to GB diffusion is more significant with decreasing temperature.

The duration of acceleration creep is proportional to the duration of transient creep as shown in Figure 11, which is described as

$$(t_r - t_m) = 2.7t_m, \qquad [7]$$

where $(t_r - t_m)$ is the duration of acceleration creep as can be seen from Figure 1 and the t_m corresponds to the duration of transient creep. Equation [7] suggests that in the acceleration creep region, the creep rate increases until the specimen ruptures after taking a time of 2.7 times the duration of transient creep. The longer duration of transient creep results in the longer duration of acceleration creep upon Eq. [7] and hence the longer time to rupture. The duration of transient creep depends on the resistance to recovery for the nucleation of soft region, while that of acceleration creep depends on the resistance to recovery for the development of soft region.

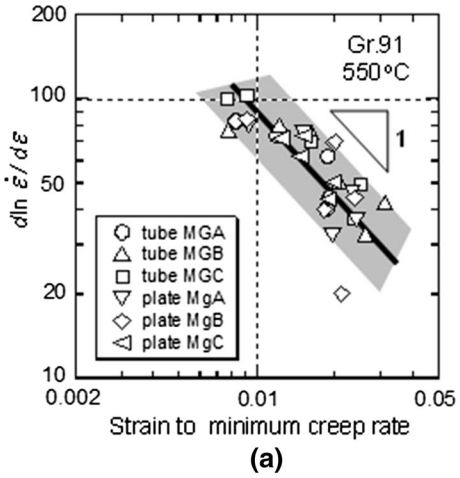

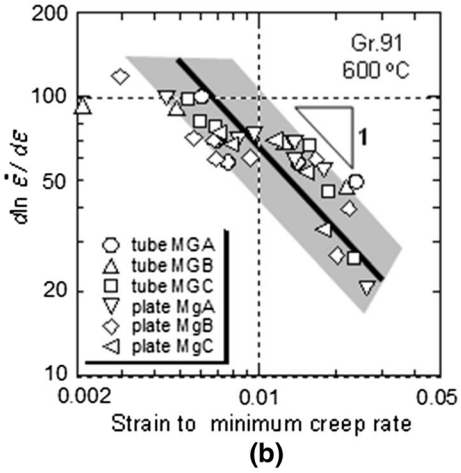

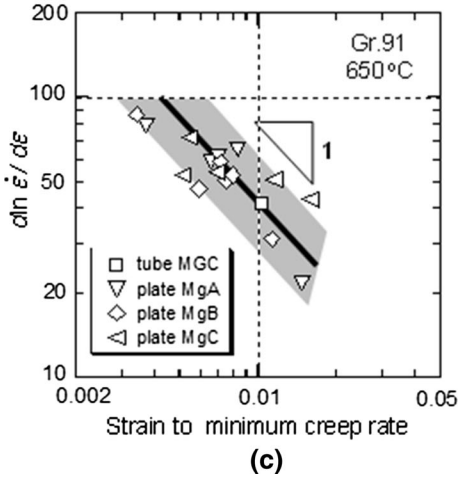

Fig. 10—Relationship between $d\ln\dot{\varepsilon}/d\varepsilon$ and strain to minimum creep rate ε_m for Gr.91 at (*a*) 823 K (550 °C), (*b*) 873 K (600 °C), and (*c*) 923 K (650 °C).

IV. CREEP LIFE EQUATION

A. *Creep Life Equation Based on Creep Behavior in Transient and Acceleration Regions*

Using the creep deformation parameters in the transient and acceleration regions, we obtain the creep life equation as

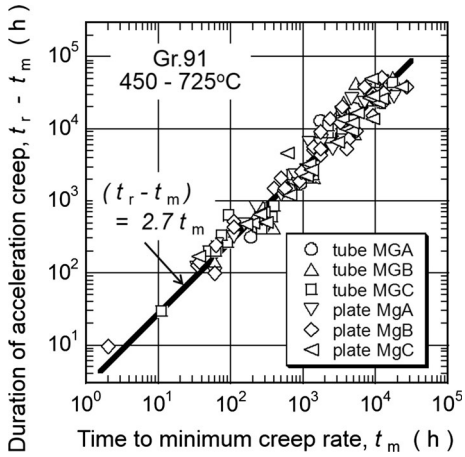

Fig. 11—Relationship between duration of acceleration creep and time to minimum creep rate for Gr.91.

$$t_r = c/[\dot{\varepsilon}_{min}(d\ln\dot{\varepsilon}/d\varepsilon)] \quad [8]$$

$$c = 1/[(t_r - t_m)/t_r]. \quad [9]$$

The derivation of Eqs. [8] and [9] is described elsewhere.[19] The constant c in Eq. [9] is an inverse of the ratio of duration of acceleration region ($t_r - t_m$) to the creep life and we obtain $c = 1.5$.[19] Eq. [8] is experimentally confirmed for Gr.91 over a wide range of test temperature and test duration, as shown in Figure 12, where the results for 9Cr-boron steel,[46] Gr.92 (9Cr-0.5Mo-1.8W-VNb steel),[47] and Gr.122 (11Cr-0.4Mo-2W-1CuVNb steel)[48] are also shown. Eq. [8] with $c = 1.5$ has already reported for tempered martensitic 9Cr-(0-4)W-0.1C steels[19,20] and austenitic steels.[43]

The present results indicate that the time to rupture is reasonably correlated with the creep deformation parameters $\dot{\varepsilon}_{min}$ and $d\ln\dot{\varepsilon}/d\varepsilon$, which reflect the creep deformation behavior in the transient and acceleration regions, respectively. This indicates that the creep life depends on the creep deformation behavior not only in the transient region but also in the acceleration region. It should be noted that the stress dependence of $\dot{\varepsilon}_{min}$ is much larger than that of $d\ln\dot{\varepsilon}/d\varepsilon$, as can be seen from Figures 2 and 9(a). This indicates that the main factor determining the stress dependence of time to rupture is the $\dot{\varepsilon}_{min}$ but not the $d\ln\dot{\varepsilon}/d\varepsilon$.

B. *Creep Life Prediction Based on Time to Minimum Creep Rate*

Although Eq. [8] provides us a reasonable equation for the creep life, it is necessary to carry out a long-term creep test for up to a later stage of acceleration region for estimation of the parameter $d\ln\dot{\varepsilon}/d\varepsilon$. In the following, the creep life is correlated with the creep deformation parameters in the transient region so that we can predict the creep life at earlier times.

The creep life consists of the duration of transient and acceleration creep. From Figure 11 and Eq. [7], showing

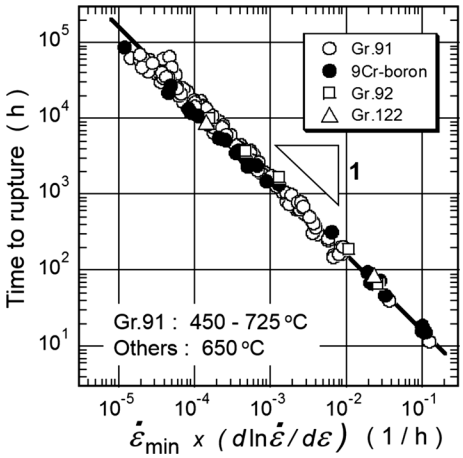

Fig. 12—Relationship between time to rupture and minimum creep rate $\dot{\varepsilon}_{min}$ times acceleration of creep rate $d\ln\dot{\varepsilon}/d\varepsilon$ in acceleration creep region for Gr.91, 9Cr-boron steel, Gr.92, and Gr.122.

t(acceleration region) = 2.7 t_m, the creep life is correlated with the t_m as[34]

$$t_r = t(\text{transient}) + t(\text{acceleration}) = 3.7t_m. \quad [10]$$

Equation [10] is also derived from the creep life equation Eq. [8]. Insertion of Eqs. [3] and [6] into Eq. [8] gives us

$$\begin{aligned} t_r &= 1.5/[\dot{\varepsilon}_{min}(d\ln\dot{\varepsilon}/d\varepsilon)] \\ &= 1.5/[\{0.54(\varepsilon_m/t_m)\}\{(0.68 \pm 0.3)/\varepsilon_m\}] \\ &\cong 3.7t_m. \end{aligned}$$

The proportional constant 3.7 = $1/(t_m/t_r)$ in Eq. [10] is an average value over a wide range of temperature [723 K to 996 K (450 °C to 725 °C)], stress (40 to 450 MPa), and test duration (t_r = 11.4 to 68,755 hours). Because the stress and temperature affect the creep deformation behavior, the stress and temperature dependence of t_m/t_r is examined. This is shown in Figure 13(a). In the temperature range between 823 K and 996 K (550 °C and 725 °C), the t_m/t_r decreases with decreasing stress and the solid line showing the stress dependence of t_m/t_r is described as

$$t_m/t_r = 1.10 \times 10^{-1} \log\sigma + 2.90 \times 10^{-3} \text{ at 40 to 100 MPa} \quad [11a]$$

$$t_m/t_r = 4.05 \times 10^{-1}\log\sigma - 5.89 \times 10^{-1} \text{ at 100 to 260 MPa}, \quad [11b]$$

where σ is the stress in MPa. The stress dependence of t_m/t_r is much smaller at low stresses below 100 MPa than at high stresses above 100 MPa. The temperature dependence of t_m/t_r is negligibly small as shown by substantially the same values of t_m/t_r at the same stresses between 823 K and 873 K (550 °C and 600 °C) and between 873 K and 923 K (600 °C and 650 °C).

Taking the stress dependence of t_m/t_r into account, the creep life is described as

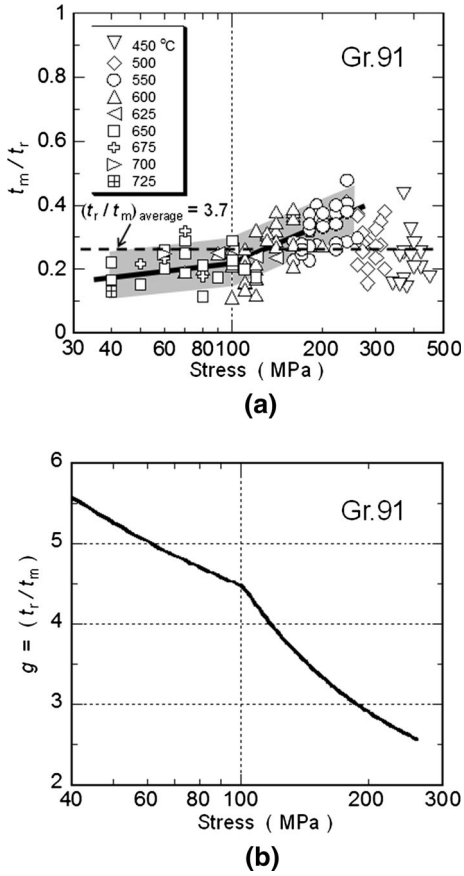

Fig. 13—Stress dependence of (*a*) t_m/t_r and (*b*) $g = (t_r/t_m)$ for Gr.91.

$$t_r = gt_m, \quad [12]$$

where g is a proportional constant given by $g = (t_r/t_m)$. The stress dependence of g is shown in Figure 13(b), which is described as

$$g = 7.734 - 7.789 \times 10^{-2}\sigma + 6.917 \times 10^{-4}\sigma^{2} - 2.376 \times 10^{-6}\sigma^{3} \text{ at 40 to 100 MPa} \quad [13a]$$

$$g = 9.611 - 7.829 \times 10^{-2}\sigma + 3.150 \times 10^{-4}\sigma^{2} - 4.550 \times 10^{-7}\sigma^{3} \text{ at 100 to 260 MPa.} \quad [13b]$$

Equation [12] is experimentally confirmed for Gr.91 over a wide range of test temperature and test duration. This is shown in Figure 14, together with the results on the other 9 to 12Cr steels of Gr.92,[47] Gr.122,[48] 9Cr-boron steel,[46] 9Cr-oxide dispersion strengthened (ODS) steel (9Cr-0.13C-2W-0.2Ti-0.35Y_2O_3),[49] 9Cr-1W steel[19] subjected to tempering and cold rolling, and A_{C3}-HAZ specimens of Gr.92,[50,51] Gr.122[48], and 9Cr-boron steel,[51] where HAZ means the heat-affected-zone of welded joints. The A_{C3}-HAZ specimens were subjected to rapid heating to A_{C3} temperature and then raid cooling to room temperature followed by

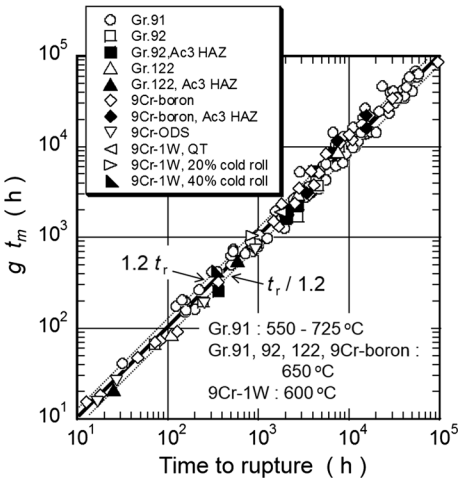

Fig. 14—Relationship between $g\ t_m$ and time to rupture for the ferritic steels.

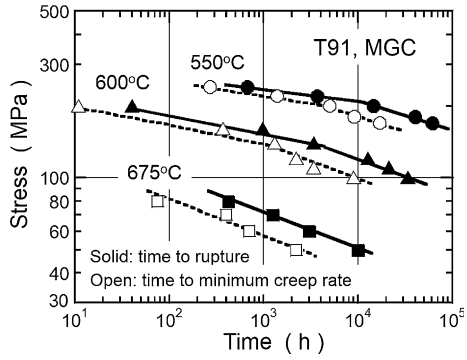

Fig. 15—Stress dependence of time to minimum creep rate t_m (open symbols) and time to rupture t_r (solid symbols) for MGC heat of T91.

post-weld heat treatment at around 1013 K (740 °C), which simulates the microstructure of HAZ of welded joints. The creep rupture strength of the A_{C3}-HAZ specimens of Gr.92 and Gr.122 was much lower than that of base metals. Eq. [12] gives us more reliable creep life prediction for Gr.91 than Eq. [10]. Using Eq. [12], the creep life of Gr.91 is predicted with an accuracy of factor of 1.2 for most of the data as shown by the dotted lines in Figure 14 by evaluating the t_m after carrying out the creep test for up to the end of transient region or for up to the initial stage of acceleration region, corresponding to less than 30 pct of the creep life, without any stress extrapolation. The life prediction factor of 1.2 means that the time to rupture can be predicted within the range from (t_r/1.2) to 1.2 t_r.

The present Gr.91 exhibits the degradation in creep rupture strength at low stresses and long times due to microstructure degradation, as shown in Figure 3. In the present method, the relationship between the t_r and t_m is described by a unique line given by Eq. [12] and the creep life is predicted without any stress and temperature extrapolation. Eq. [12] suggests that the t_m exhibits the same stress dependence as the t_r. This indicates that the stress dependence of t_m predicts an inflection point in the stress rupture data and also predicts the degradation in creep rupture strength at long times, as shown in Figure 15. It should be also noted that the heat-to-heat variation in time to rupture among the different heats of present Gr.91 is rather large as shown by much shorter t_r of the heats MgA and MgB than the other heats, as shown in Figure 3. Again, in the present method, the t_r is predicted by Eq. [12], irrespective of strong or weak heats. The strong heats exhibit large t_m, while the weak heats exhibit small t_m. Kobayashi and co-workers observed the presence of δ-ferrite in the initial microstructure of the weak heat MgB before the creep test but not in the strong heat MgC.[52]

If the t_m is predicted at early times in the transient creep region before reaching a minimum creep rate, the creep life can be predicted at a time earlier than t_m.

V. PREDICTION OF TOTAL STRAIN

Figure 16 shows the total strain in creep rupture testing for tubes and plates of Gr.91 at 823 K, 873 K, and 923 K (550 °C, 600 °C, and 650 °C), as a function of time to rupture. The total strain maintains high values of 20 to 40 pct for up to about 10,000 hours and then decreases with increasing test duration at 823 K and 873 K (550 °C and 600 °C), while it decreases continuously from short times of about 100 hours to long times of about 100,000 hours at a high temperature of 923 K (650 °C).

The total strain consists of the strain accumulated in the transient region, corresponding to ε_m, and the strain accumulated in the acceleration region, corresponding to ($\varepsilon_r - \varepsilon_m$), where ε_r is the total strain, as shown schematically in Figure 1. The ε_m is much smaller than the ε_r, as shown by ε_m = 0.2 to 3 pct in Figure 5 and ε_r = 10 to 60 pct in Figure 16. This indicates that the total strain substantially consists of the strain accumulated in the acceleration region. The $d\ln\dot{\varepsilon}/d\varepsilon$ is inversely proportional to the ε_m as shown in Figure 10, while the total strain is inversely proportional to the $d\ln\dot{\varepsilon}/d\varepsilon$ as can be seen from Figure 1. Therefore, the total strain would be proportional to the ε_m. Figures 17(a) and (b) show the relationship between the total strain and $d\ln\dot{\varepsilon}/d\varepsilon$ and the relationship between the total strain and ε_m, respectively, at 823 K, 873 K, and 923 K (550 °C, 600 °C, and 650 °C). The total strain is inversely proportional to the $d\ln\dot{\varepsilon}/d\varepsilon$ with the exception of some data points at 923 K (650 °C), Figure 17(a). In Figure 17(b), the total strain increases with increasing ε_m but the linear relationship is not seen. The ε_m dependence of total strain is larger at a higher temperature of 923 K (650 °C) than that at 823 K and 873 K (550 °C and 600 °C). As already described in Figure 8, the creep strain significantly increases just before the creep rupture due to necking. In the present paper, the effect of necking is not taken into account in the evaluation of $d\ln\dot{\varepsilon}/d\varepsilon$, as the $d\ln\dot{\varepsilon}/d\varepsilon$ was evaluated from the constant portion of $d\ln\dot{\varepsilon}/d\varepsilon$ in the acceleration region shown in Figure 8. This seems to be the main reason for the lack of a linear relationship

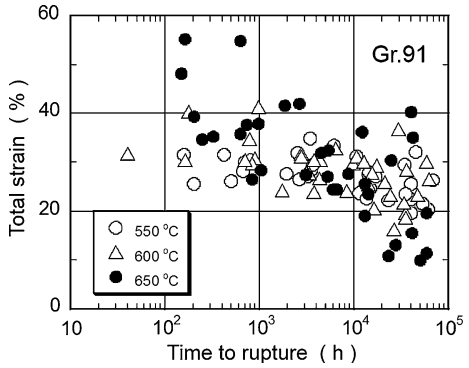

Fig. 16—Total strain of Gr.91 at 823 K, 873 K, and 923 K (550 °C, 600 °C, and 650 °C).

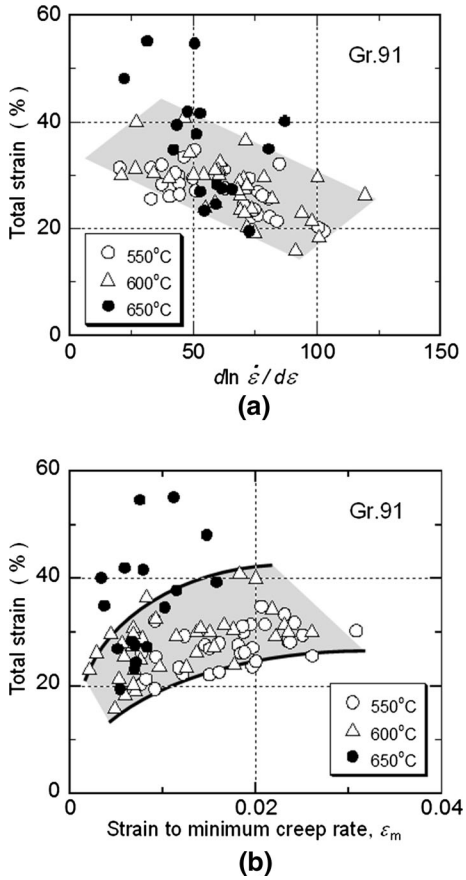

Fig. 17—(*a*) Relationship between total strain and $d\ln\dot{\varepsilon}/d\varepsilon$ in the acceleration creep region and (*b*) relationship between total strain and strain to minimum creep rate ε_m for Gr.91 at 823 K, 873 K, and 923 K (550 °C, 600 °C, and 650 °C).

between the total strain and ε_m. The contribution of necking to the total strain becomes more significant with increasing stress, namely, with increasing ε_m, because the reduction of area in creep rupture testing increases with increasing stress.[24,25] The incorporation of necking effect in the prediction of total strain is a future problem. Nevertheless, using the results in Figure 17(b), the total strain is predicted by evaluating the ε_m after carrying out the creep test for up to the end of transient region or for

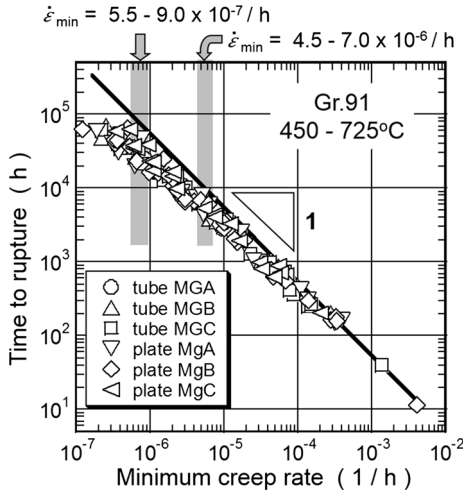

Fig. 18—Relationship between time to rupture and minimum creep rate for Gr.91.

up to the initial stage of acceleration region, similar as the prediction of creep life by evaluating the t_m. On the other hand, the creep life equation given in Eq. [8] containing the term of $d\ln\dot{\varepsilon}/d\varepsilon$ and the creep life prediction based on Eq. [12] are reasonable, because the linear part of the creep rate *vs* strain curves in the acceleration region corresponds to larger than 90 pct of the acceleration region in the creep strain *vs* time curves even at a low stress of 100 MPa, as shown in Figure 8(b), even if the creep strain significantly increases just before the creep rupture.

VI. ORIGIN OF DEVIATION FROM MONKMAN–GRANT RELATIONSHIP

Traditionally, the Monkaman–Grant relationship[53] described as

$$t_r = (c'/\dot{\varepsilon}_{min})^{m'}, \qquad [14]$$

where c' and m' are constants, has been used for the prediction of creep life of heat-resistant steels. Usually, the m' is smaller than 1. Figure 18 shows the Monkman–Grant plot for Gr.91 at 723 K to 998 K (450 °C to 725 °C). At short-time conditions, corresponding to the t_r shorter than about 500 hours, the t_r is inversely proportional to the $\dot{\varepsilon}_{min}$ as $t_r = c'/\dot{\varepsilon}_{min}$ and $m' = 1$. The constant c' is given by 5.2×10^{-2}. At long-time conditions, corresponding to the t_r longer than about 500 hours, however, the relationship between the t_r and $\dot{\varepsilon}_{min}$ deviates downward, indicating $m' < 1$ in Eq. [14], although the upper limit of time to rupture data in Figure 18 is still described by the Eq. [14] with $c' = 5.2 \times 10^{-2}$ and $m' = 1$. The downward deviation means that even if the minimum creep rate decreases to 1/10 of the original value, the time to rupture does not increase 10 times. It should be also noted that the difference between the maximum and minimum t_r at the same $\dot{\varepsilon}_{min}$ becomes more significant with decreasing stress and increasing test duration.

The downward deviation showing $m' < 1$ was also observed for P91 by Choudhary.[54] He carried out creep rupture testing for P91 at 793 K and 873 K (520 °C and 600 °C) for up to about 10,000 hours and showed the downward deviation at long times above 500 to 1000 hours at 873 K. He pointed out that the downward deviation is due to an effect of thermal instability of the secondary phase particles such as $M_{23}C_6$ and MX, which loss their pinning efficiency for long time of exposure, and make easier recovery.

Based on the relationship between the t_r and creep deformation parameters described in the previous sections, let us consider the reason why the downward deviation takes place in the Monkman–Grant plot in Figure 18 and the reason why the difference between the maximum and minimum t_r at the same $\dot{\varepsilon}_{min}$ becomes more significant with decreasing stress and increasing test duration.

Figure 19 shows the relationship between the ε_m and t_m at approximately the same $\dot{\varepsilon}_{min}$ of (5.5 to 9.0) $\times 10^{-7}$/h and (4.5 to 7.0) $\times 10^{-6}$/h shown by gray-colored bands in Figure 18. The t_r varies from 2×10^4 to 7×10^4 hours and from 3×10^3 to 9×10^3 hours at the $\dot{\varepsilon}_{min}$ of (5.5 to 9.0) $\times 10^{-7}$/h and (4.5 to 7.0) $\times 10^{-6}$/h, respectively. In Figure 19, both the ε_m and t_m change upon the condition of $\varepsilon_m \propto t_m$ or $(\varepsilon_m/t_m) =$ constant, as can be seen from Eq. [3]. Figures 20(a) and 20(b) show the relationship between the t_r and t_m and the relationship between t_r and ε_m, respectively, at the same $\dot{\varepsilon}_{min}$. The t_r increases linearly with increasing t_m, as can be seen from Eq. [12]. The t_r also increases linearly with increasing ε_m, because the t_m increases upon $t_m \propto \varepsilon_m$ at the same $\dot{\varepsilon}_{min}$ as shown in Figure 19. Therefore, the t_r widely varies at the same $\dot{\varepsilon}_{min}$ as shown in Figure 20, because the t_m and ε_m change upon $t_m \propto \varepsilon_m$ and the t_r is proportional to the t_m. Figure 21(a) shows a set of schematic creep curves having same $\dot{\varepsilon}_{min}$ but different t_r. In spite of the same $\dot{\varepsilon}_{min}$, the t_r of the creep curve (2) shown by the dotted line is half of that of the creep curve (1) shown by the solid line. When both the t_m and ε_m of the creep curve (2) are half of those of the creep curve (1), the $\dot{\varepsilon}_{min}$ of the creep curve (2) is the same as that of the creep curve (1) as can be seen from Eq. [3], but the t_r of the creep curve (2) is half of that of the creep curve (1), because the t_r is proportional to the t_m. The smaller ε_m of the creep curve (2) than the creep curve (1) results in smaller total or rupture elongation ε_r. Figure 21(b) compares the three creep curves having same $\dot{\varepsilon}_{min}$ and same transient creep region but different t_r. The same transient creep region means the same t_m and ε_m, which results in the same acceleration region and hence the same t_r and ε_r. Because $t_r = g\ t_m$, where g depends on stress and an average value of g is 3.7, the creep curve (3) is reasonable but not the creep curves (4) and (5). It is concluded that the variation of t_r at the same $\dot{\varepsilon}_{min}$ in the Monkman–Grant plot in Figure 18 results from the variation of t_m and ε_m, as shown in Figure 20.

Next, let us consider the reason why the downward deviation takes place at low stresses and long times in the Monkman–Grant plot in Figure 18, indicating $m' < 1$ in Eq. [14]. Figures 22(a) and (b) show the relationship between the t_m and $\dot{\varepsilon}_{min}$ and the relationship between the ε_m and $\dot{\varepsilon}_{min}$, respectively, for the heat MgB of Gr.91 at 773 K to 923 K (500 °C to 650 °C). At a low temperature of 773 K (500 °C), the t_m is inversely

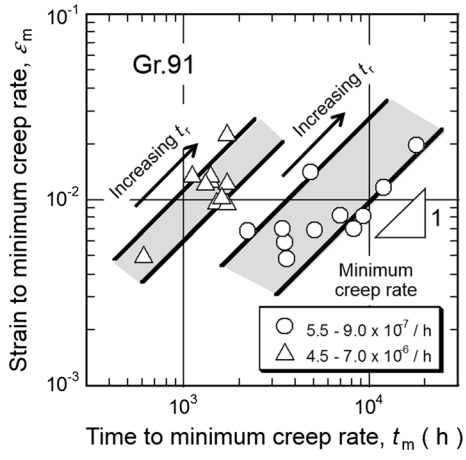

Fig. 19—Relationship between strain to minimum creep rate ε_m and time to minimum creep rate t_m at the same minimum creep rates for Gr.91.

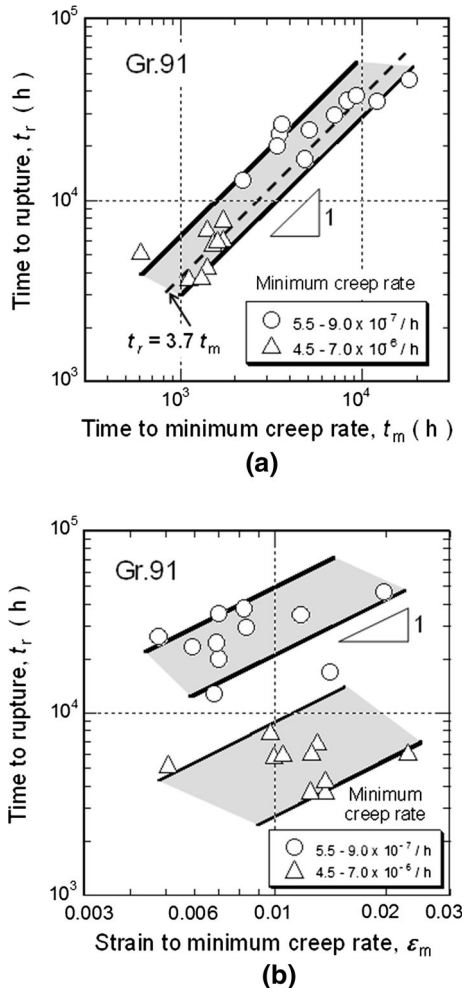

Fig. 20—(*a*) Relationship between t_r and ε_m and (*b*) relationship between t_r and t_m at the same minimum creep rates for Gr.91.

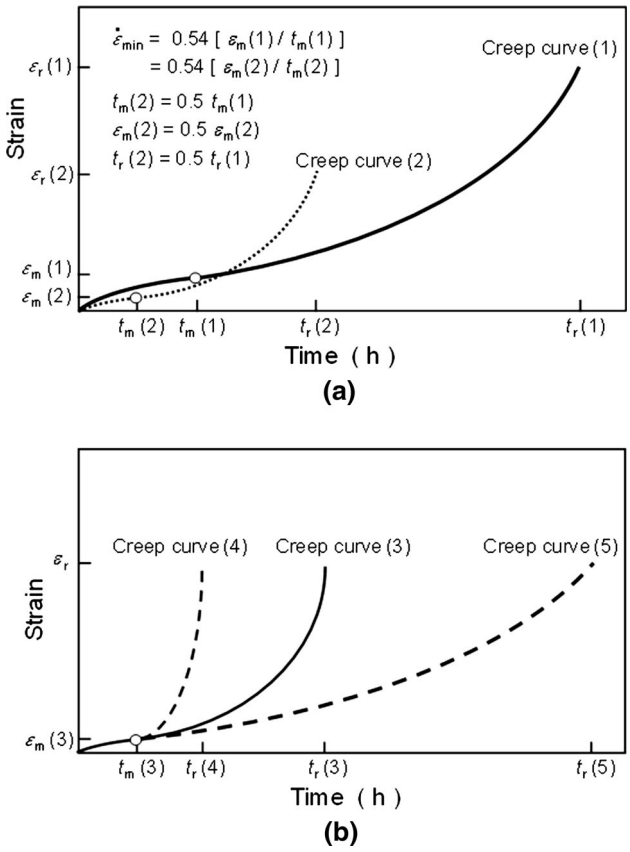

Fig. 21—(*a*) Schematic creep curves having same $\dot{\varepsilon}_{min}$ but different t_m, ε_m, and t_r and (*b*) schematic creep curves having same $\dot{\varepsilon}_{min}$ and transient region but different t_r.

proportional to the $\dot{\varepsilon}_{min}$ for up to long times of about $t_m = 3 \times 10^4$ hours, which corresponds to the t_r of 6.5×10^4 hours in Figure 18, while the ε_m is approximately constant but does not decrease with decreasing $\dot{\varepsilon}_{min}$. The downward deviation of the t_m *vs* $\dot{\varepsilon}_{min}$ curves in Figure 22(a) becomes more significant with increasing temperature from 773 K to 873 K (500 °C to 600 °C) and then it saturates at around 923 K (650 °C). The downward deviation of the t_m *vs* $\dot{\varepsilon}_{min}$ curves reflects the downward deviation of the Monkman–Grant plot in Figure 18, because the t_r is proportional to the t_m. The decrease in ε_m with decreasing $\dot{\varepsilon}_{min}$ in Figure 22(b) is correlated with the downward deviation of the t_m *vs* $\dot{\varepsilon}_{min}$ curves in Figure 22(a), because the decrease in ε_m is concomitant with the decrease in t_m at the same $\dot{\varepsilon}_{min}$, Eq. [3]. The present analysis suggests that the downward deviation of the t_r *vs* $\dot{\varepsilon}_{min}$ curves (Monkman–Grant plot) in Figure 18 is caused by the decrease in ε_m with decreasing stress, indicating a significant change in ε_r from large values at high stresses to low values at low stresses. At a low temperature of 773 K (500 °C), the creep tests were carried out only at high stress conditions of 240 to 320 MPa as shown in Figure 5. This results in no downward deviation of the t_m *vs* $\dot{\varepsilon}_{min}$ curves and the t_r *vs* $\dot{\varepsilon}_{min}$ curves, Monkman–Grant plot in Figure 18.

Figure 23 compares the t_r *vs* $\dot{\varepsilon}_{min}$ curves for Gr.91, comparing with several ferritic steels. Of the steels, the

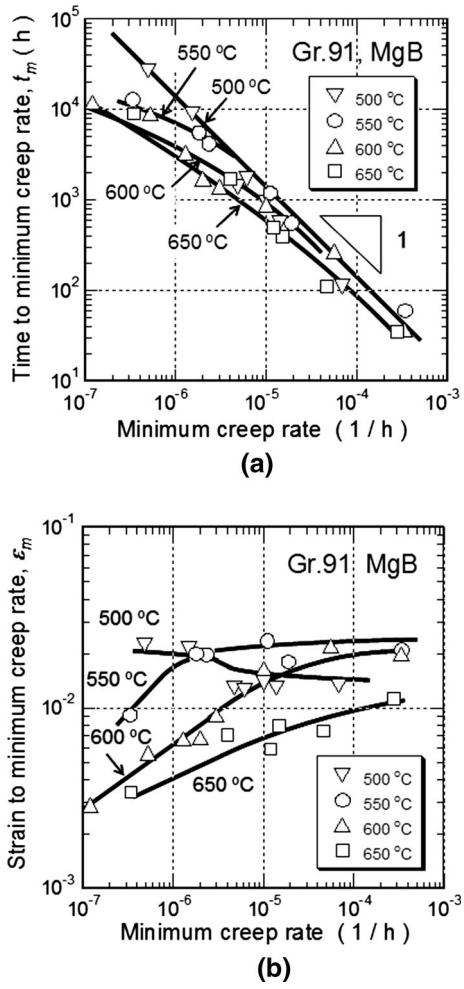

Fig. 22—(*a*) Relationship between t_m and $\dot{\varepsilon}_{min}$ and (*b*) relationship between ε_m and $\dot{\varepsilon}_{min}$ for heat MgB of Gr.91.

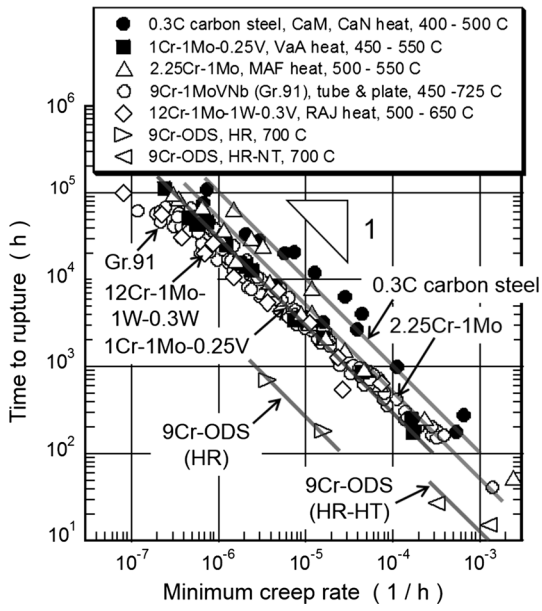

Fig. 23—Relationship between time to rupture and minimum creep rate for the ferritic steels.

Table II. Constant c' for Monkman–Grant Relationship Eq. [14]

Steel	c'
0.3C Carbon steel	1.12×10^{-1}
1Cr-1Mo-0.25V	3.19×10^{-2}
2.25Cr-1Mo	4.75×10^{-2}
9Cr-ODS (HR)	2.62×10^{-3}

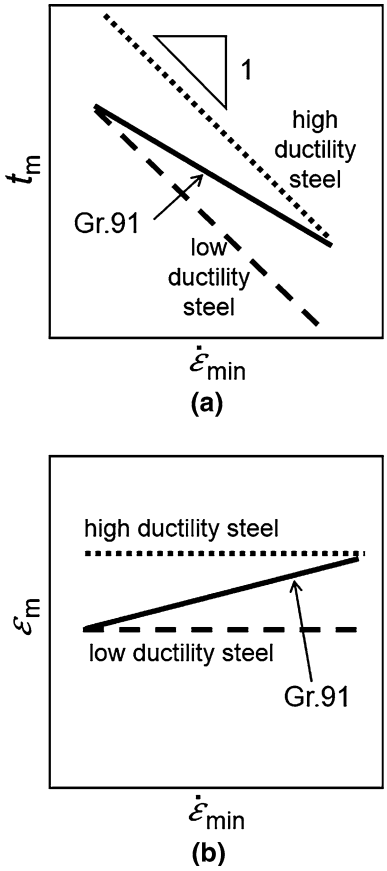

Fig. 24—Schematics of (*a*) relationship between t_m and $\dot{\varepsilon}_{min}$ and (*b*) relationship between ε_m and $\dot{\varepsilon}_{min}$.

0.3C carbon steel,[55] 1Cr-1Mo-0.25V steel[56] having martensitic microstructure, 2.25Cr-1Mo steel[57] having ferritic and pearlitic microstructure, and 9Cr-ODS steel[49] having martensitic microstructure show that the t_r is inversely proportional to the $\dot{\varepsilon}_{min}$ and $m' = 1$ in Eq. [14]. The constant *c'* in Eq. [14] is given in Table II. The 0.3C carbon and 2.25Cr-1Mo steels are high ductility steels having large ε_r for a wide range of test temperatures and stresses, suggesting no significant decrease in ε_m with stress and hence $m' = 1$, as shown schematically in Figure 24. The 1Cr-1Mo-0.25V and 9Cr-ODS steels, which are significantly strengthened by fine MX carbonitrides and fine oxides, respectively, are low ductility steels having small ε_r for a wide range of test temperatures and stresses, suggesting no significant decrease in ε_m with stress and hence $m' = 1$, as shown schematically in Figure 24. The 12Cr-1Mo-1W-0.3V steel[58] having martensitic microstructure behaves similar as Gr.91, $m' < 1$, namely large ε_r at high stresses but small ε_r at low stresses. Gr.92[59] and Gr.122,[60] which are martensitic 9Cr and 12Cr steels, respectively, also behave similar as Gr.91, $m' < 1$.

VII. CONCLUSIONS

1. The minimum creep rate $\dot{\varepsilon}_{min}$ is inversely proportional to the time to minimum creep rate t_m, while it is proportional to the strain to minimum creep rate ε_m as given by

$$\dot{\varepsilon}_{min} = 0.54(\varepsilon_m / t_m).$$

   The strain to minimum creep rate ε_m decreases with decreasing stress, suggesting that the creep deformation becomes localized in the transient region at low stresses. This hypothesis agrees with the observation of preferential or localized recovery of martensitic microstructure in the vicinity of PAGBs in Gr.91 by Kushima and co-workers[36] after creep rupture testing for 34,141 hours at 873 K (600 °C) and 100 MPa.
2. In the acceleration region, the $d\ln\dot{\varepsilon}/d\varepsilon$ mainly consists of the parameter n (stress exponent of $\dot{\varepsilon}_{min}$) at high stresses, indicating that the acceleration of creep rate results from an increase in stress by a decrease in cross section with strain under constant load conditions. At low stresses, on the other hand, the $d\ln\dot{\varepsilon}/d\varepsilon$ mainly consists of the microstructure degradation parameter m and inhomogeneous creep deformation parameter i. The duration of acceleration region is proportional to the t_m, while the $d\ln\dot{\varepsilon}/d\varepsilon$ is inversely proportional to the ε_m.
3. The creep life is described as

$$t_r = c/[\dot{\varepsilon}_{min}(d\ln\dot{\varepsilon}/d\varepsilon)],$$

   where $\dot{\varepsilon}_{min}$ and $d\ln\dot{\varepsilon}/d\varepsilon$ reflect the creep behavior in the transient and acceleration regions, respectively. The main factor determining the stress dependence of time to rupture is the $\dot{\varepsilon}_{min}$ but not the $d\ln\dot{\varepsilon}/d\varepsilon$. The creep life is also correlated with the t_m as

$$t_r = g t_m.$$

   The constant g slightly increases with decreasing stress. Using the later equation, we can reasonably predict the creep life of Gr.91 by evaluating the t_m after carrying out the creep test for up to the end of transient region or for up to the initial stage of acceleration region, corresponding to less than 30 pct of the creep life, without any stress extrapolation. The present equation also predicts the degradation in creep strength at low stresses and also the heat-to-heat variation in t_r at earlier times.

4. The total strain is inversely proportional to the $d\ln\dot{\varepsilon}/d\varepsilon$ in the acceleration region, while it increases with increasing ε_m but the linear relationship between the total strain and ε_m is not seen. Using the results on the relationship between the total strain and ε_m, the total strain is predicted by evaluating the ε_m after carrying out the creep test for up to the end of transient region or for up to the initial stage of acceleration region, similar as the prediction of creep life by evaluating the t_m.
5. The relationship between the t_r and $\dot{\varepsilon}_{min}$, called Monkman–Grant relationship, deviates downward at low stresses and long times at temperatures above 823 K (550 °C). The difference between the maximum and minimum t_r at the same $\dot{\varepsilon}_{min}$ becomes more significant with decreasing stress and increasing test duration. The downward deviation of the t_r *vs* $\dot{\varepsilon}_{min}$ curves (Monkman–Grant plot) is caused by the decrease in ε_m with decreasing stress. At the same $\dot{\varepsilon}_{min}$, the decrease in ε_m is concomitant with the decrease in t_m upon $t_m \propto \varepsilon_m$ and the t_r is proportional to the t_m.
6. The 0.3C carbon steel and 2.25Cr-1Mo steel, which are high ductility steels having large ε_r for a wide range of test temperature and stress, and the 1Cr-1Mo-0.25V steel and 9Cr-ODS steel, which are low ductility steels having small ε_r for a wide range of test temperature and stress, exhibit no downward deviation of the t_r *vs* $\dot{\varepsilon}_{min}$ curves. The martensitic 12Cr-1Mo-1W-0.3V steel behaves similar as Gr.91, as shown by the downward deviation of the t_r *vs* $\dot{\varepsilon}_{min}$ curves.

NOMENCLATURE

σ	Stress (MPa)
ε	Strain
$\dot{\varepsilon}$	Creep rate (h^{-1})
$\dot{\varepsilon}_{min}$	Minimum creep rate (h^{-1})
ε_m	Creep strain to minimum creep rate
$d\ln\dot{\varepsilon}/d\varepsilon$	Increase in creep rate by strain in acceleration region
t_m	Time to minimum creep rate (h)
t_r	Time to rupture or creep life (h)
ε_r	Total or rupture strain
c, c'	Constants
g	Constant

REFERENCES

1. F. Abe: *Curr. Opin. Solid State Mater. Sci.*, 2004, vol. 8, pp. 305–11.
2. F. Abe: in *Structural Alloys for Power Plants*, A. Shirzadi and S. Jackson, eds., Woodhead Publishing Limited, Cambridge, 2014, pp. 250–93.
3. T. Allen, H. Burlet, R.K. Nanstad, M. Samaras, and S. Ukai: *MRS Bull.*, 2009, vol. 34 (1), pp. 1–8.
4. F. Abe: in *Coal Power Plant Materials and Life Assessment*, A. Shibli, ed., Woodhead Publishing Limited, Cambridge, 2014, pp. 3–51.
5. F. Abe: *Int. J. Press. Vessels Pip.*, 2008, vol. 85 (1), pp. 99–107.
6. S.R. Holdsworth and G. Merckling: *Proc. of the 6th Intern. Charles Parsons Turbine Conf.*, 16–18 September 2003, Dublin, Ireland, 2003, pp. 411–26.
7. G. Merckling: *Int. J. Press. Vessels Pip.*, 2008, vol. 85 (1), pp. 2–13.
8. W. Bendick, L. Cipolla, J. Grabel, and J. Hald: *Int. J. Press. Vessels Pip.*, 2010, vol. 87 (3), pp. 304–09.
9. B. Wilshire and P.J. Scharning: *Int. Mater. Rev.*, 2008, vol. 53, pp. 91–104.
10. K. Kimura: *Proc. of ASME 2004 Pressure Vessels & Piping Conference (PVP2005)*, July 17–21, 2005, Denver, CO, 2005, PVP2005-71039.
11. H.G. Armaki, K. Maruyama, M. Yoshizawa, and M. Igarashi: *Mater. Sci. Eng. A*, 2008, vol. 490 (1), pp. 66–71.
12. F. Abe: in *Creep-Resistant Steels*, F. Abe, T.-U. Kern, and R. Viswanathan, eds., Woodhead Publishing Limited, Cambridge, England, 2008, pp. 3–14.
13. F. Masuyama and N. Nishimura: *Proc. of the 10th International Conference on Strength of Materials*, Sendai, Japan, August 21–26, 1994, pp. 657–60.
14. I. Nonaka: *Proc. of 3rd Intern. ECCC Conf. on Creep & Fracture in High temperature Components & Life Assessment*, May 5–7, 2014, Rome, Italy, 2014, Paper No. 36.
15. M. Prager: *J. Pressure Vessel Technol.*, 1995, vol. 117 (5), pp. 95–103.
16. H. Semba, B. Dyson, and M. McLean: *Proc. of Intern. Conf. on Creep & Fracture in High Temperature Components*, September 12–14, 2005, London, 2005, pp. 419–27.
17. R. Lim, M. Sauzay, F. Dalle, I. Tournie, P. Bonnaillie, and A. Gourgues-Lorenzon: *Int. J. Fract.*, 2011, vol. 169, pp. 213–28.
18. F. Abe: *Metall. Trans. A*, 1995, vol. 26A, pp. 2237–46.
19. F. Abe: *Metall. Mater. Trans. A*, 2003, vol. 34A, pp. 913–25.
20. F. Abe: *Metall. Mater. Trans. A*, 2005, vol. 36A, pp. 321–32.
21. K. Kimura, H. Kushima, and F. Abe: *Proc. EPRI Intern. Conf. on Advances in Life Assessment and Optimization of Fossil Power Plants*, Orlando, FL, March 11–13, 2002, pp. 1–17.
22. K. Kimura, K. Sawada, K. Kubo, and H. Kushima: *ASME PVP*, 2004, vol. 476, pp. 11–18.
23. K. Kimura, K. Sawada, and H. Kushima: *ASME PVP2010*, July 18–22, 2010, Bellevue, Washington, PVP2010-25297, 2004, pp. 1–10.
24. NIMS Creep Data Sheets, Atlas of Creep Deformation Property, No. D-1, Tokyo, Tsukuba, National Institute for Materials Science, 2007.
25. NIMS Creep Data Sheets, Atlas of Creep Deformation Property, No. D-2, Tokyo, Tsukuba, National Institute for Materials Science, 2008.
26. R. Wu, R. Sandström, and J. Storesund: *Mater. High Temp.*, 1994, vol. 12, pp. 277–83.
27. F. Abe, S. Nakazawa, H. Araki, and T. Noda: *Metall. Trans. A*, 1992, vol. 23A, pp. 469–77.
28. F. Abe and S. Nakazawa: *Metall. Trans. A*, 1992, vol. 23A, pp. 3025–34.
29. R.W. Evans and B. Wilshire: *Creep of Metals and Alloys*, The Institute of Metals, London, 1985, pp. 114–53.
30. J. Cadek: *Creep in Metallic Materials*, Elsevier, Amsterdam, 1988, pp. 115–59.
31. L. Kloc and V. Sklenicka: *Mater. Sci. Eng. A*, 1997, vols. 234–236, pp. 962–65.
32. J.C.M. Li: *Acta Metall.*, 1963, vol. 11 (11), pp. 1269–70.
33. S. Yamasaki, M. Mitsuhara, K. Ikeda, S. Hata, and H. Nakashima: *Tetsu-to-Hagane*, 2014, vol. 100 (5), pp. 688–95.
34. S. Spigarelli, L. Kloc, and P. Bontempi: *Scripta Mater.*, 1997, vol. 37 (4), pp. 399–404.
35. F. Abe: *Int. J. Mater. Res.*, 2012, vol. 103 (6), pp. 765–73.
36. H. Kushima, K. Kimura, and F. Abe: *Tetsu-to-Hagane*, 1999, vol. 85(11), pp. 841–47, in Japanese.
37. J. Hald: *Int. J. Press. Vessels Pip.*, 2008, vol. 85, pp. 30–37.
38. T. Shrestha, M. Basirat, I. Charit, G.P. Potirniche, K.K. Rink, and U. Sahaym: *J. Nucl. Mater.*, 2012, vol. 423, pp. 110–19.
39. S. Spigarelli: *Int. J. Press. Vessels Pip.*, 2013, vol. 101, pp. 64 71.

40. S. Straub, M. Meier, J. Ostermann, and W. Blum: *VGB Kraftw*., 1993, vol. 73 (8), pp. 646–53.
41. F. Abe: *Mater. Sci. Eng. A*, 1997, vols. 234–236, pp. 1045 48.
42. F. Abe: *Mater. Sci. Eng. A*, 2001, vols. 319–321, pp. 770–73.
43. E. Baba, O. Kanemaru, F. Abe, and K. Yagi: *Tetsu-to-Hagane*, 1995, vol. 81(8), pp. 845–50, in Japanese.
44. K. Maruyama, K. Sawada, and J. Koike: *ISIJ Int*., 2001, vol. 41 (6), pp. 641–53.
45. K. Sawada, H. Kushima, M. Tabuchi, and K. Kimura: *Mater. Sci. Eng. A*, 2011, vol. 528A, pp. 5511–18.
46. F. Abe: *Int. J. Mater. Res*., 2008, vol. 99 (4), pp. 387–94.
47. K. Sawada, K. Kubo, and F. Abe: *Mater. Sci. Eng. A*, 2001, vols. 319–321, pp. 784–87.
48. F. Abe and M. Tabuchi: *Mater. Sci. Technol. Weld. Join*., 2004, vol. 9 (1), pp. 22–30.
49. S. Ukai, R. Miyata, X. Wu, Y. Sugino, N. Oono, S. Hayashi, E. Maeda, T. Azuma, S. Ohtsuka, and T. Kaito: *Proc. of 12th Intern. Conf. on Creep and Fracture of Eng. Mater. and Structures*, May 2012, Kyoto, CD-ROM, 2012.
50. Y. Liu, S. Tsukamoto, T. Shirane, and F. Abe: *Metall. Mater. Trans. A*, 2013, vol. 44A, pp. 4626–33.
51. Y. Liu, S. Tsukamoto, K. Sawada, and F. Abe: *Metall. Mater. Trans. A*, 2014, vol. 45A, pp. 1306–14.
52. S. Kobayashi, K. Sawada, T. Hara, H. Kushima, and K. Kimura: *Mater. Sci. Eng. A*, 2014, vol. 592, pp. 241–48.
53. F.C. Monkaman and N.J. Grant: *Proc. ASTM*, 1956, vol. 56, pp. 593–620.
54. B.K. Choudhary: *Mater. Sci. Eng. A*, 2013, vol. A585, pp. 1–9.
55. NIMS Creep Data Sheets, No. 17B, Tokyo, Tsukuba, National Institute for Materials Science, 1994.
56. NIMS Creep Data Sheets, No. 9B, Tokyo, Tsukuba, National Institute for Materials Science, 1990.
57. NIMS Creep Data Sheets, No. 3B, Tokyo, Tsukuba, National Institute for Materials Science, 1986.
58. NIMS Creep Data Sheets, No. 10B, Tokyo, Tsukuba, National Institute for Materials Science, 1998.
59. NIMS Creep Data Sheets, No. 48A, Tokyo, Tsukuba, National Institute for Materials Science, 2012.
60. NIMS Creep Data Sheets, No. 51A, Tokyo, Tsukuba, National Institute for Materials Science, 2013.